Electronic Supplementary Material (ESI) for Journal of Materials Chemistry A.

Supporting Information

Biomimetic, Multifunctional, Superhydrophobic Graphene Film with Self-Sensing and Fast Recovery for Microdroplet Transportation

Guomin Ding, Weicheng Jiao*, Rongguo Wang, Yue Niu, Lifeng Hao, Fan Yang, Wenbo Liu

Science and Technology on Advanced Composites in Special Environments Laboratory, Harbin Institute of Technology, Harbin 150080, P. R. China

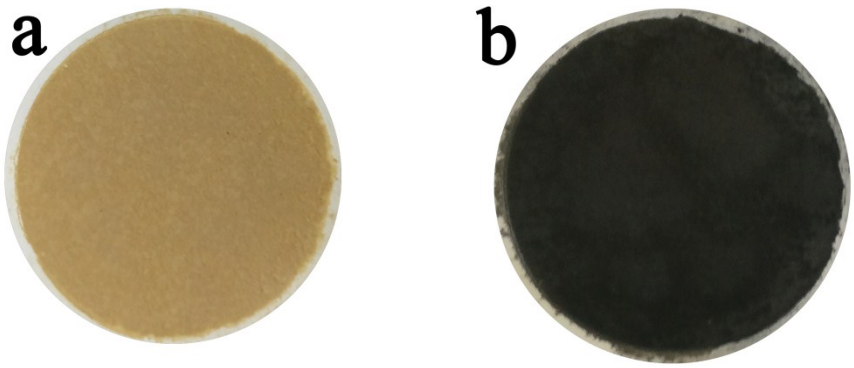

Fig. S1 Digital images of the closed-cell GO and rGO film. a) GO film, b) rGO film.

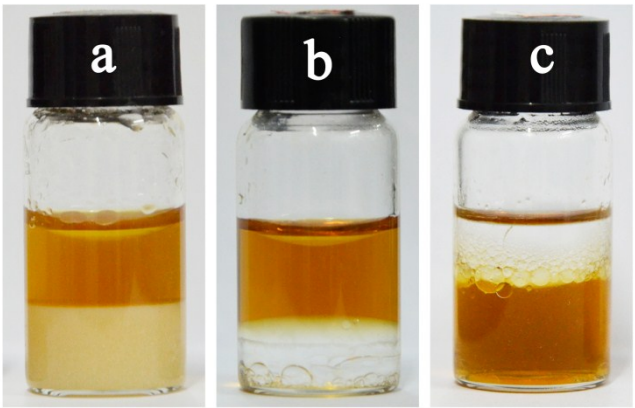

Fig. S2 GO Pickering emulsion prepared using different oil phases at the same rotational speed of 8 kr/min. a) DE-in-GO solution Pickering emulsion. b) Dichloromethane-in-GO solution Pickering emulsion. c) n-Heptane-in-GO solution Pickering emulsion.

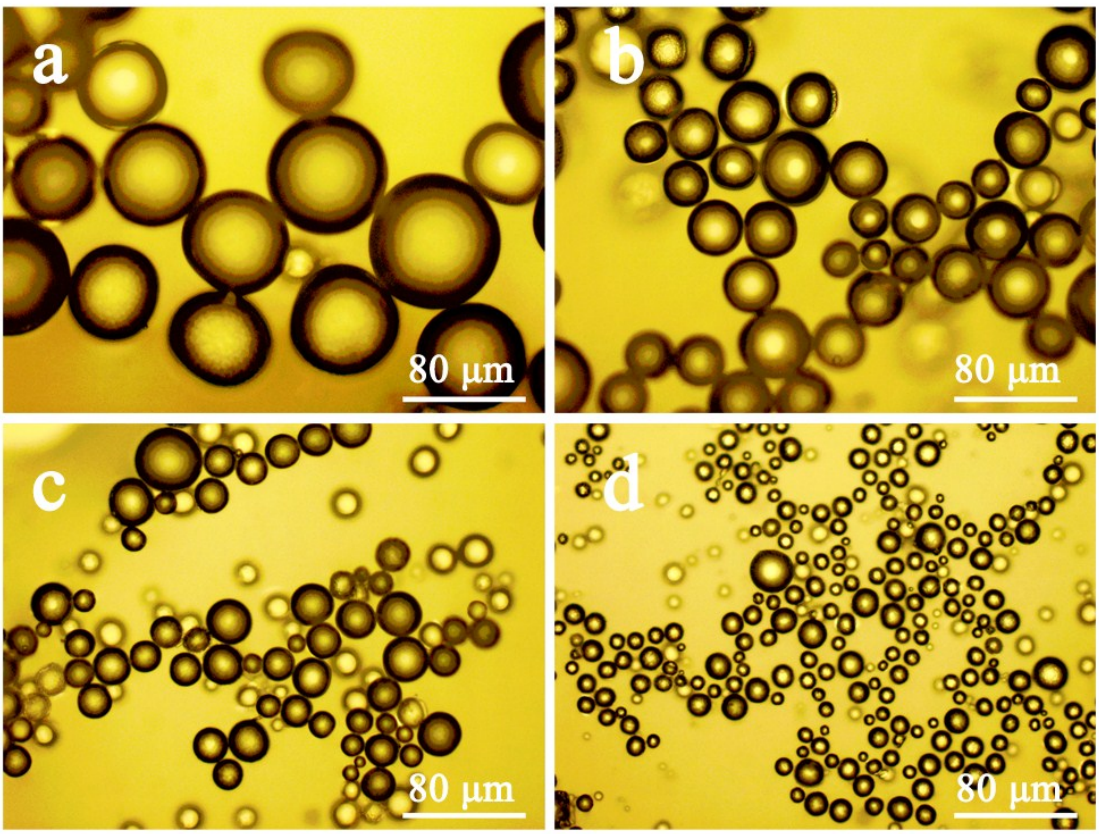

Fig. S3 Optical micrographs of the frozen emulsions. a-d) Ordinal micrographs of frozen DGPE-8, DGPE-12, DGPE-16 and DGPE-20.

Fig.S4 The change in volume of the liquid and frozen DE. a) The volume of liquid DE. b) The volume of frozen DE.

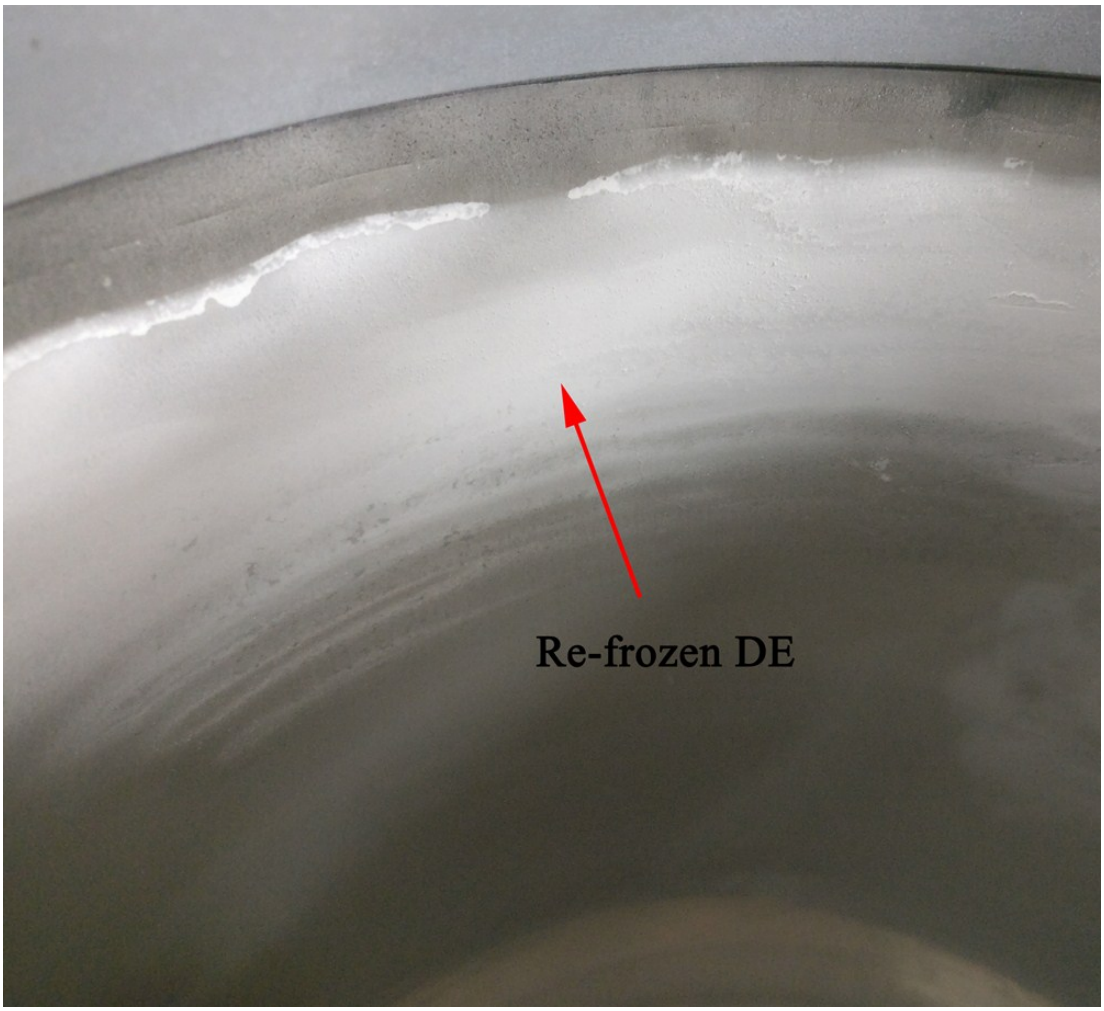

Fig. S5 Photograph of re-frozen DE on the surface of the freeze-dryer's cold trap.

Table S1. Recovery rate of DE after freeze-drying.

The quality of DE in the pristine films (g)	The quality of recovered DE (g)	Recovery rate
1.9314	1.7695	91.6%

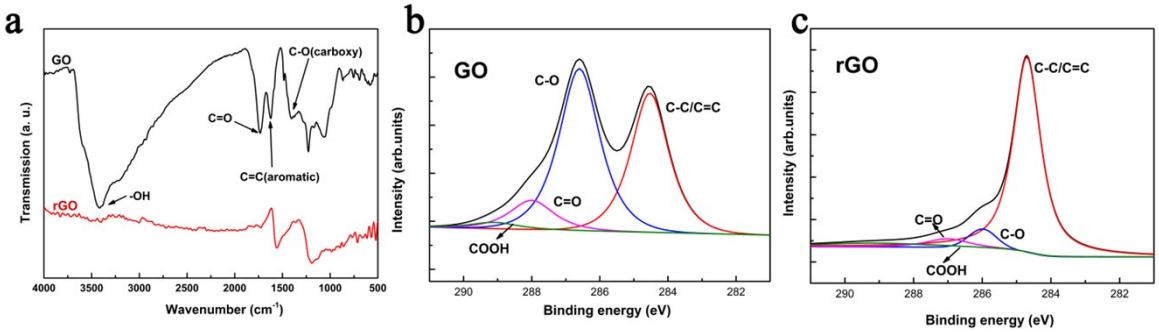

Fig. S6 The chemical characteristics of the GO and rGO films. a) FTIR spectra, b,c) C1 s spectra of XPS.

In the FTIR spectra, the peaks of GO at 3420 cm^{-1}, 1725 cm^{-1}, 1392 cm^{-1} and 1230 cm^{-1} correspond to the O-H, C=O, carboxy C-O and hydroxyl/epoxy C-O stretching vibrations, respectively (Fig. S6a). [1-3] However, in the case of rGO, these peaks almost disappear. In the XPS spectra, the double peak structure of the C1 s spectra of GO and rGO can be deconvoluted into four chemically shifted components at 284.6, 286.6, 288.0, and 289.1 eV, which are attributed to the C–C/C=C, C–O, C=O, and COOH functional groups, respectively (Fig. S6b, c).[4, 5] The most obvious difference is the atomic ratio of the carbon/oxygen ratio. Due to the removal of oxygen groups, the carbon/oxygen ratio of rGO equals 8.1, which is larger than that of GO (2.5). All of these changes indicate that the GO has been successfully reduced to graphene.

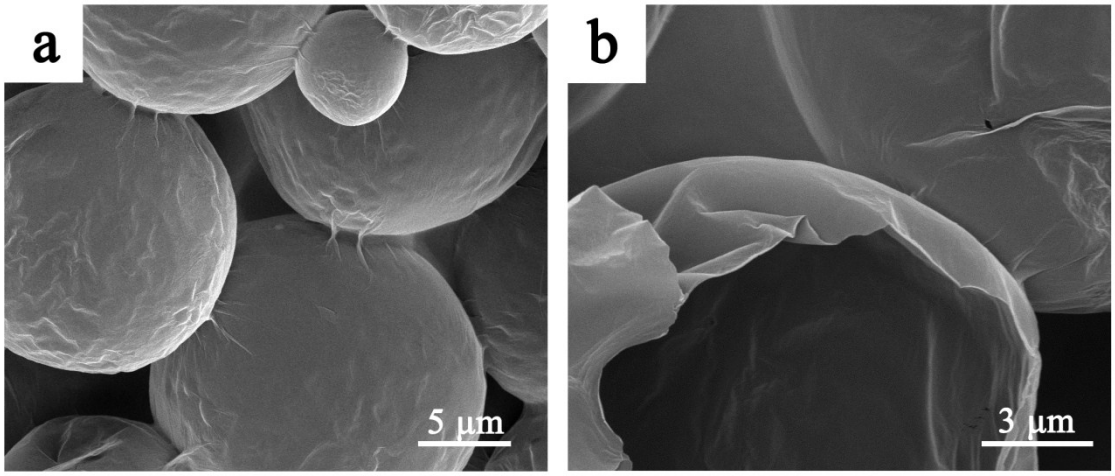

Fig. S7 SEM images of the connections and hollow structures of the graphene cells. a) The graphene connection between the cells of CCGF-16. b) Broken cell in CCGF-16.

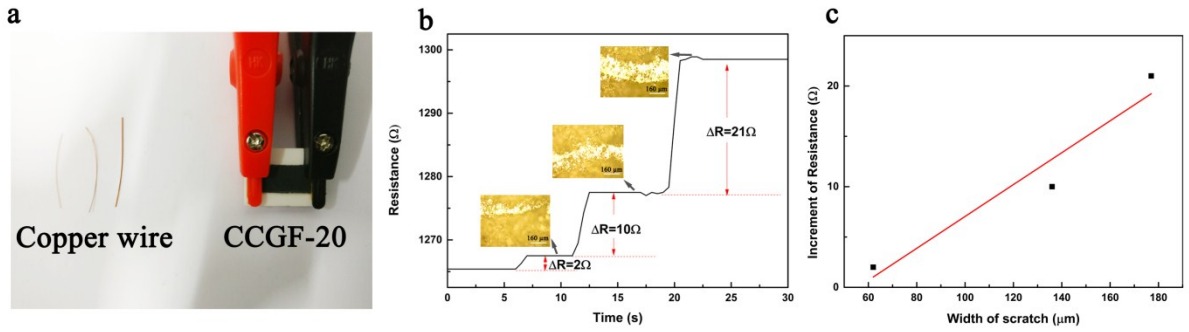

Fig. S8 Response of the CCGF-20 to scratches. a) The photograph of copper wire with different thickness and the CCGF-20. b). Resistance change in CCGF-20 with scratches. Insets are the micrographs of different scratch. c). Increment of resistance as a function of the width of scratch and the fitting line

The increment in the resistance (ΔR) was detected when the different scratch was generated by scratching with the different copper wire in Fig. S8a. During scratching the film, we guaranteed that the length of every scratch was same. By the micrographs, we got the width of scratches which was 68 μm, 136 μm and 177μm respectively (insets of Fig S8b). As the scratches appeared in ascending order, the ΔR increased at a near linear trend. So based on the increment of resistance, the CCGF-20 can recognize the extent of scratch.

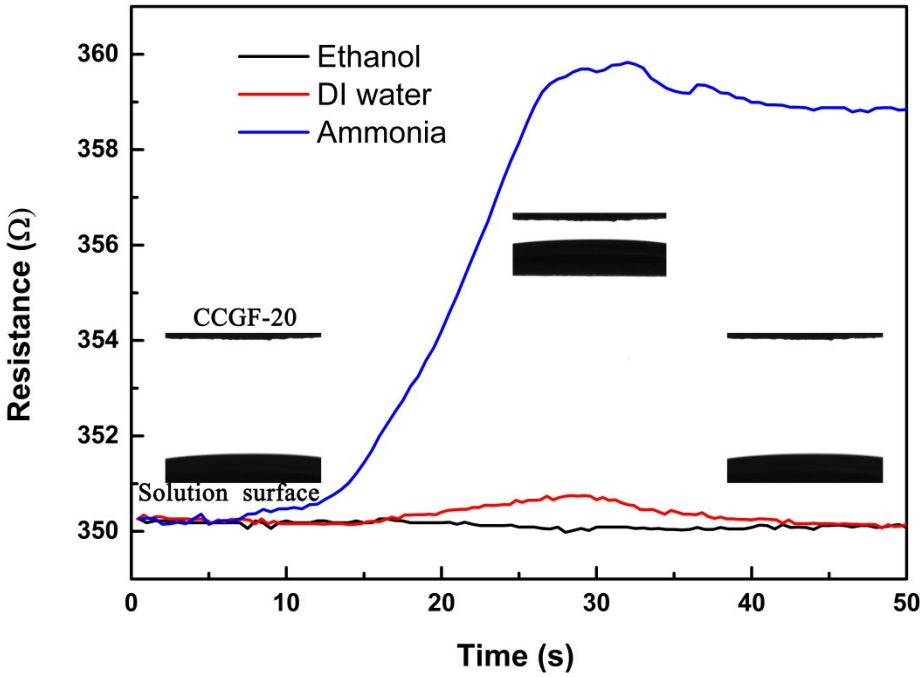

Fig.S9 Change in the resistance of CCGF-20 closing to a different solution. Inset contains the images of different spaces between CCGF-20 and the solution surface.

The change in the resistance was detected when a different solution was near CCGF-20. There was almost no change in the resistance when ethanol approached CCGF-20. However, the resistance increased when water moved closer to the graphene film, and the resistance decreased as the water moved away. In addition, the resistance of the graphene film increased sharply when it was near ammonia (concentration of 25%～28%). The obvious distinction in the increment of resistance is attributed to the sensitivity of graphene for different vapors.[6, 7] However, the resistance of CCGF-20 did not return to its initial resistance when ammonia was removed because ammonia has a greater adsorption energy on graphene nanosheets than water molecules. [8, 9] Therefore, the desorption of ammonia molecules cannot be achieved naturally.

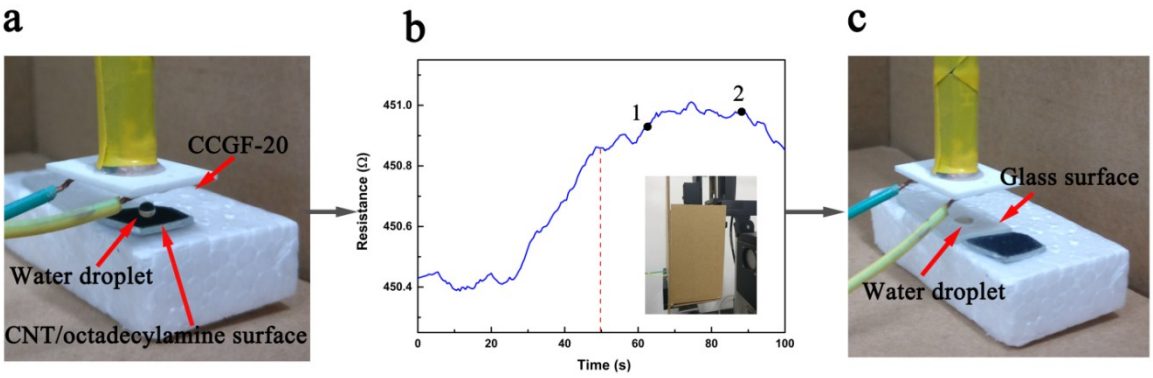

Fig. S10 The microdroplet transportation without video observation. a). The water droplet is located on the superhydrophobic surface. b). The change of resistance for microdroplet transportation without video observation. c). The water droplet had been transferred to glass surface.

The microdroplet transportation without video observation was showed in the Fig. S10. First, the CNT/octadecylamine superhydrophobic surface with the water droplet (6μL) and the glass surface were placed in an opaque box on a lifting platform (Fig. S10a). The CCGF-20 was above CNT/octadecylamine surface. Then, the box was closed (inset of Fig. S10b) and the resistance was detected. As the platform was risen at a speed of 0.1 mm/s, the resistance increased gradually from ~ 450.42 Ω. After the time point of about 50s, slope of curve, which could be evaluated by comparison of adjacent multiple points, decreased obviously and we considered the water droplet just touched CCGF-20 at this time. But in order to ensure the graphene film contacting the water droplet sufficiently, we lowered the platform at following point 1. At that moment, we believed the water droplet had contacted with the graphene film enough because the slope of curve still was small. Then, platform was lowered by 4 mm. After the retracting of platform, the resistance of film remained at 450.97 Ω. This confirmed that the water droplet had been picked up by CCGF-20. Next, the platform was moved so that the glass surface is below the CCGF-20 and then risen by 4 mm (point 2 of Fig. S10b). The resistance decreased slowly. This indicated the

water drop had been transferred to glass surface. The photograph of the water drop on the glass surface had also confirmed the success of transportation (Fig. S10c).

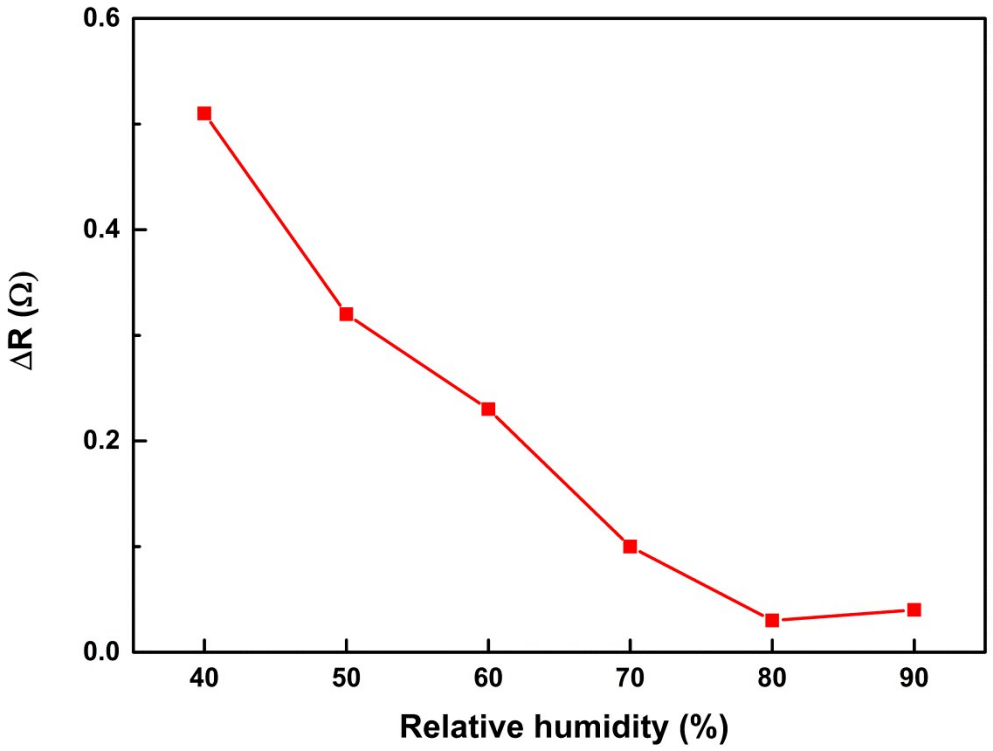

Fig. S11 The influence of environmental humidity on the self-sensing performance of CCGF-20.

The capability of self-sensing of CCGF-20 has been explored in the different environmental relative humidity at room temperature (Fig. S11). Δ R is the difference of the resistance of stage 3 and the resistance of stage 1, which is used to characterize the self-sensing performance. As shown in Fig. S11, as the humidity increased, Δ R decreased gradually from 0.51 Ω at the relative humidity of 40% to 0.04 Ω at the relative humidity of 90%. This phenomenon indicated the self-sensing of CCGF-20 was becoming degraded with the increasing humidity. This is due to the fact that as the humidity increases, the initial adsorption amount of water vapor molecules increases.

When the water droplet approaches to the graphene film in high humidity environment, the final increment of water molecules decreases so that the increase of resistance is less obvious. When the humidity reaches 80% and even more, the initial water molecule reaches the saturation nearly. So though water drop approaches to the film, the adsorption amount of water molecules is not increased and the resistance hardly changes.

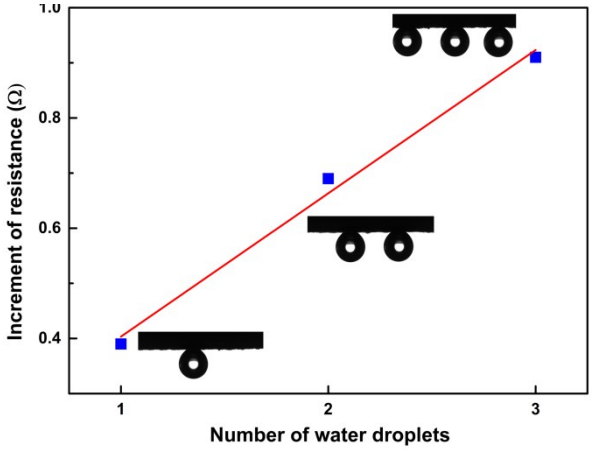

Fig.S12 Increment of resistance as a function of the number of water droplets and the fitting line. Insets were the images of different number of water droplets on the CCGF-20 surfaces in the microdroplet transportation.

Increment of resistance was measured when different number of water droplets was picked up by CCGF-20 in the microdroplet transportation. The water droplets with same volume (3 μL) were lined up. The result shows that as the number of droplets increases, the increment of resistance increases at a near linear trend. We consider this phenomenon could be explained by the adsorption amount of water vapor molecules. Because of the same size of droplets, the projection area of multiple droplets multiplies on graphene film. When approaching the droplets, the adsorption amount of water molecules also multiplies so that the increment of resistance

increases linearly. So by detecting the extent of increment of resistance, the number of droplets on the surface can be counted.

Notes and references

1 S. Park, K.-S. Lee, G. Bozoklu, W. Cai, S. T. Nguyen and R. S. Ruoff, ACS nano, 2008, 2, 572-578.
2 D. C. Marcano, D. V. Kosynkin, J. M. Berlin, A. Sinitskii, Z. Sun, A. Slesarev, L. B. Alemany, W. Lu and J. M. Tour, ACS nano, 2010, 4, 4806-4814.
3 J. Chen, B. Yao, C. Li and G. Shi, Carbon, 2013, 64, 225-229.
4 C. Mattevi, G. Eda, S. Agnoli, S. Miller, K. A. Mkhoyan, O. Celik, D. Mastrogiovanni, G. Granozzi, E. Garfunkel and M. Chhowalla, Advanced Functional Materials, 2009, 19, 2577-2583.
5 R. Gusain, H. P. Mungse, N. Kumar, T. R. Ravindran, R. Pandian, H. Sugimura and O. P. Khatri, J. Mater. Chem. A, 2016, 4, 926-937.
6 F. Schedin, A. Geim, S. Morozov, E. Hill, P. Blake, M. Katsnelson and K. Novoselov, Nature materials, 2007, 6, 652-655.
7 A. Lipatov, A. Varezhnikov, P. Wilson, V. Sysoev, A. Kolmakov and A. Sinitskii, Nanoscale, 2013, 5, 5426-5434.
8 L. Guo, H.-B. Jiang, R.-Q. Shao, Y.-L. Zhang, S.-Y. Xie, J.-N. Wang, X.-B. Li, F. Jiang, Q.-D. Chen, T. Zhang and H.-B. Sun, Carbon, 2012, 50, 1667-1673.
9 Y. Peng and J. Li, Frontiers of Environmental Science & Engineering, 2013, 7, 403-411.